Contribution of Ryanodine Receptor Type 3 to Ca^{2+} Sparks in Embryonic Mouse Skeletal Muscle

Matthew W. Conklin,* Virginia Barone,# Vincenzo Sorrentino,#§ and Roberto Coronado*
*Department of Physiology, University of Wisconsin, Madison, WI 53706; #DIBIT San Raffaele Scientific Institute, Milan, Italy; and §Dipartimento di Scienze Biomediche, Università degli Studi di Siena, Siena, Italy

ABSTRACT The kinetic behavior of Ca^{2+} sparks in knockout mice lacking a specific ryanodine receptor (RyR) isoform should provide molecular information on function and assembly of clusters of RyRs. We examined resting Ca^{2+} sparks in RyR type 3-null intercostal myotubes from embryonic day 18 (E18) mice and compared them to Ca^{2+} sparks in wild-type (wt) mice of the same age and to Ca^{2+} sparks in fast-twitch muscle cells from the foot of wt adult mice. Sparks from RyR type 3-null embryonic cells (368 events) were significantly smaller, briefer, and had a faster time to peak than sparks from wt cells (280 events) of the same age. Sparks in adult cells (220 events) were infrequent, yet they were highly reproducible with population means smaller than those in embryonic RyR type 3-null cells but similar to those reported in adult amphibian skeletal muscle fibers. Three-dimensional representations of the spark peak intensity ($\Delta F/Fo$) vs. full width at half-maximal intensity (FWHM) vs. full duration at half-maximal intensity (FTHM) showed that wt embryonic sparks were considerably more variable in size and kinetics than sparks in adult muscle. In all cases, tetracaine (0.2 mM) abolished Ca^{2+} spark activity, whereas caffeine (0.1 mM) lengthened the spark duration in wt embryonic and adult cells but not in RyR type 3-null cells. These results confirmed that sparks arose from RyRs. The low caffeine sensitivity of RyR type 3-null cells is entirely consistent with observations by other investigators. There are three conclusions from this study: i) RyR type-1 engages in Ca^{2+} spark activity in the absence of other RyR isoforms in RyR type 3-null myotubes; ii) Ca^{2+} sparks with parameters similar to those reported in adult amphibian skeletal muscle can be detected, albeit at a low frequency, in adult mammalian skeletal muscle cells; and iii) a major contributor to the unusually large Ca^{2+} sparks observed in normal (wt) embryonic muscle is RyR type 3. To explain the reduction in the size of sparks in adult compared to embryonic skeletal muscle, we suggest that in embryonic muscle, RyR type 1 and RyR type 3 channels co-contribute to Ca^{2+} release during the same spark and that Ca^{2+} sparks undergo a maturation process which involves a decrease in RyR type 3.

INTRODUCTION

Ryanodine receptor (RyR) channels are ultimately responsible for the transient elevation of cytosolic Ca^{2+} following muscle cell depolarization. Of the three RyR isoforms described in various tissues, RyR type 1 and RyR type 3 have been shown to be expressed in skeletal muscles of several species (Oyamada et al., 1994; Sutko and Airey, 1996; Conti et al., 1996; Sorrentino and Reggiani, 1999). RyR type 3 shares ~67% identity with the major adult skeletal RyR isoform (type 1) and ~70% identity with the cardiac RyR isoform (type 2) (Hakamata et al., 1992). RyR type 3 is abundantly expressed in the adult brain in the corpus striatum, hippocampus, and frontal and parietal cortex (Hakamata et al., 1992; Giannini et al., 1995). In addition, RyR type 3 transcripts have been detected in adult smooth muscles, heart, testis, and spleen (Hakamata et al., 1992; Giannini et al., 1995).

RyR type 1 plays a central role in voltage-dependent activation of Ca^{2+} release. This isoform interacts closely with the dihydropyridine receptor (DHPR) and both complexes are colocalized in junctional domains formed by the sarcoplasmic reticulum (SR) and t-system membranes (Block et al., 1988). RyR type 1 channels activated by the depolarized DHPR are directly responsible for the initiation of the Ca^{2+} transient during skeletal-type EC coupling. However, RyR type 3 cannot substitute for RyR type 1 in this function (Yamazawa et al., 1997; Takeshima et al., 1995; Bertocchini et al., 1997). This led to the suggestion that RyR type 3 may participate in the amplification of Ca^{2+} release after cytosolic Ca^{2+} is increased by other means (Takeshima et al., 1995; Bertocchini et al., 1997). Some ligand gating characteristics of RyR type 3 channels lend support to this hypothesis. Increasing free Ca^{2+} in the micromolar range produces a steep steady-state activation of RyR type 3 channels with a Hill coefficient of ~2.7 (Sonnleitner et al., 1998) which is much higher than that reported for RyR type 1 or type 2 channels (Gyorke et al., 1994). In addition, the activity of RyR type 3 channels does not decline with free Ca^{2+} in the millimolar range, suggesting that RyR type 3 channels are less sensitive to Ca^{2+}-dependent inactivation than RyR type 1 channels (Sonnleitner et al., 1998). Based on these characteristics, it has been speculated that during a global Ca^{2+} transient, when the free Ca^{2+} reaches the micromolar range, activation of RyR type 3 channels may prolong the transient (Sonnleitner et al., 1998). However, global Ca^{2+} transients measured by whole-cell fura-2 fluorescence in cultured myotubes from the diaphragm of control (wt) and RyR type 3-null mice were not significantly different (Dietze et al., 1998). Thus,

Received for publication 18 March 1999 and in final form 27 May 1999.
Address reprint requests to Roberto Coronado, Department of Physiology, University of Wisconsin, 1300 University Avenue, Madison, WI 53706. Tel.: 608-263-7487; Fax: 608-265--5512; E-mail: coronado@physiology.wisc.edu.

0006-3495/99/09/1394/10 $2.00

the role of RyR type 3 in the excitation-contraction coupling of adult skeletal muscle remains to be thoroughly elucidated.

The functional consequences of a secondary Ca^{2+} release system in mammalian skeletal muscle are unknown. In mice, RyR type 3 protein has been detected in all skeletal muscles of limbs and thorax investigated so far starting at embryonic day 18 (E18) and up to day 15 after birth (P15) (Bertocchini et al., 1997; Flucher et al., 1998). At later stages of development there is a severe decline in RyR type 3, which is most noticeable in the fast-twitch muscles. However, in soleus and diaphragm, RyR type 3 was detected throughout development, although there was a decline in the content of RyR type 3 at P60 relative to P15 (Bertocchini et al., 1997; Flucher et al., 1998). Hence, the impact of RyR type 3 on muscle cell function appears to be restricted mostly to events during muscle embryogenesis and to some skeletal muscles in the adult animal. The contribution of RyR type 3 to muscle cell signaling has been addressed using RyR type 1 or RyR type 3 knockout mice (Takeshima et al., 1994, 1996; Bertocchini et al., 1997; Barone et al., 1998). In RyR type 1-null myotubes in culture, RyR type 3 was shown to be expressed (Takeshima et al., 1995). In these cells, SR Ca^{2+} release in response to increases in cyotosolic Ca^{2+} and caffeine were depressed (Takeshima et al., 1995). In RyR type 3-null myotubes, on the other hand, the caffeine sensitivity of neonatal but not adult myotubes was severely depressed (Bertocchini et al., 1997). It is entirely possible that at some stages of myogenesis, a co-contribution of RyR types 1 and 3 to Ca^{2+} signaling may be essential, such that a loss of either isoform leads to a loss of the sensitivity of the remaining RyRs to Ca^{2+} and other ligands.

The concerted opening and closing of a small number of RyR channels result in a miniature Ca^{2+} release event called a spark with highly stereotypic properties (Cheng et al., 1993; Tsugorka et al., 1995; Shacklock et al., 1995; Klein et al., 1996). The kinetic behavior of sparks in knockout mice lacking DHPR subunits has provided molecular information on specific arrangements of DHPRs and RyRs underlying sparks in these cells (Conklin et al., 1999a). Ca^{2+} sparks occur at resting potentials in adult amphibian (Klein et al., 1996) and embryonic mammalian skeletal muscle (Conklin et al., 1999a). Because RyR type 3 is abundantly expressed throughout the mammalian embryonic skeletal musculature, RyR type 3 channels could augment the dimensions of Ca^{2+} sparks in embryonic muscle cells. If this is the case, Ca^{2+} sparks in embryonic muscles should differ in wt mice and RyR type 3-null mice. Furthermore, both should differ from Ca^{2+} sparks in adult wt fast-twitch muscle, in which RyR type 3 is known to be reduced, if not absent. In the present study, both hypotheses were tested. We found that spontaneous Ca^{2+} sparks were highly abundant in RyR type 3-null myotubes, demonstrating that RyR type 3 is not essential for Ca^{2+} spark occurrence. The Ca^{2+} spark parameters suggested that RyR type 3 has a pronounced contribution to these miniature Ca^{2+} release events at the embryonic stage of muscle cell development. Some of these results were previously published in abstract form (Conklin et al., 1999b).

MATERIALS AND METHODS

Single cell preparations

Embryonic myotubes were freshly isolated from intercostal muscles of embryonic day 18 (E18) wild-type (wt) and E18 RyR type 3-null mice as described (Strube et al., 1996). The two half-ribcages of each embryo were dissected in normal Krebs solution containing 136 mM NaCl, 5 mM KC1, 2 mM $CaCl_2$, l mM $MgCl_2$, and 10 mM HEPES, titrated to pH 7.4 with NaOH. The ribcages were incubated at 37°C for 10 min in phosphate buffered saline (Sigma Chemical Co., St. Louis, MO) containing collagenase (3 mg/ml, Type I, Sigma) and trypsin (1 mg/ml, Type III, Sigma). Single myotubes were obtained by mechanical dispersion of enzyme-treated ribcages in Krebs solution. Isolated cells were allowed to settle in a culture dish with its bottom replaced by a thin glass coverslip for at least 1 hour before imaging. Adult cells were freshly dissociated from the flexor digitorum brevis (FDB) muscle of 90-day-old (P90) or older mice as described (Allard et al., 1996). The plantar aponeurosis tendon that attaches the FDB to the posterior end of the foot was cut and the FDB was dissected away from the underlying fascia. The flexor tendons that attach the FDB to the anterior end of the foot were then cut to remove the entire FDB muscle. The FDB and attached tendons were incubated for 60 min without shaking in 1 ml of phosphate buffered saline (Sigma) containing 6 mg/ml collagenase Type I (Sigma) at 37°C. Single cells from collagenase-treated FBD were obtained by mechanical dispersion as described above for embryonic cells. Embryonic and adult cells were viable for several hours as demonstrated by their ability to maintain a relatively constant resting fluorescence and to contract in response to caffeine and field stimulation. The total number of cells imaged was >500 cells from adult FBD muscle preparations and >250 cells from intercostal muscle preparations from each type of embryo. The total number of cells from which sparks were collected were 26 adult cells from 22 adult mice, 56 cells from 26 type 3-null embryos, and 129 cells from 27 wt embryos. In any one preparation of cells, a minimum of 20 cells was imaged.

Ca^{2+} spark measurements

Cells were loaded with 4 μM of fluo-3 acetoxymethyl (AM) ester (Molecular Probes, Eugene, OR) for 30 min at room temperature in Krebs solution. During imaging, cells were kept in Krebs solution without fluo-3 AM at room temperature. Cells were viewed with an inverted microscope with a 40× oil immersion objective (N.A. = 1.3). The confocal attachment was an Olympus Fluoview (Olympus, Melville, NY), described elsewhere (Conklin et al., 1999a). A 5-mW Argon laser was attenuated to 6% with neutral density filters. The pixel size was 0.2 × 0.2 microns and the line-scan rate was 2.05 ms per 512-pixel line. Ca^{2+} sparks were identified in 2-D images and afterwards acquired in line-scan mode as described (Conklin et al., 1999a). A single event corresponded to a transient elevation in intensity larger than 0.3 ΔF/Fo units with a full spatial width greater than 1 micron and a full duration longer than 10 ms and less than 350 ms. The full duration was the time interval during which the fluorescence remained elevated >0.3 ΔF/Fo units above the mean baseline fluorescence. With these criteria, the smallest Ca^{2+} spark that could be possibly identified would have a full spatial width of 5 pixels, a full duration of 5 pixels, and a fluorescence intensity 30% above the average resting intensity of the image. The fluorescence intensity, F, was calculated by densitometric scanning of Ca^{2+} sparks in line-scan images. To improve the signal-to-noise ratio, F was averaged over 10 spatial pixels nearest to the center of sparks. The fluorescence intensity, Fo, was averaged in the same manner from areas of the same image without sparks. The fluorescence unit ΔF/Fo was constructed by subtracting unity from the ratio F/Fo. A compressed 32-color table and an 8-pixel running average (smoothing) was applied to

all images to highlight the center of the spark. For t-tubule visualization, cells were kept in Krebs solution with 4 μM Di-8-ANNEPS (Molecular Probes) at all times. Confocal imaging of di-8-ANNEPS fluorescence was performed with the 40× objective described above using the Argon laser for dye excitation.

Chemicals

Stock solutions of fluo-3 AM and di-8-ANNEPS (Molecular Probes) were prepared in dimethylsulfoxide. Stock solutions of tetracaine and caffeine (Sigma) were 4 mM and 10 mM, respectively, and were prepared in glass-distilled water.

RESULTS

The top images of Fig. 1 show sections of resting embryonic and adult cells stained with fluo-3 in Krebs solution containing 2 mM Ca^{2+} at room temperature. All experiments were performed under these experimental conditions in cells with a low resting cytosolic Ca^{2+} concentration as inferred from a minimal fluo-3 fluorescence. The images show sites of transient Ca^{2+} elevation due to sparks identified during repetitive scans. The insets next to each cell correspond to the same area of the cell without the spark. On average, no more than 20% of the embryonic cells and 5% of adult cells in a given preparation produced Ca^{2+} sparks under the chosen experimental conditions. Typically, embryonic cells had 1 to 3 simultaneously active sites per cell, whereas in adult cells the number of sites per cell was invariably 1. The integrity of the plasma and t-system membrane of the isolated cells was verified in the bottom panels of Fig. 1 using the fluorescent cell-impermeant dye Di-8 ANNEPS (Shack-

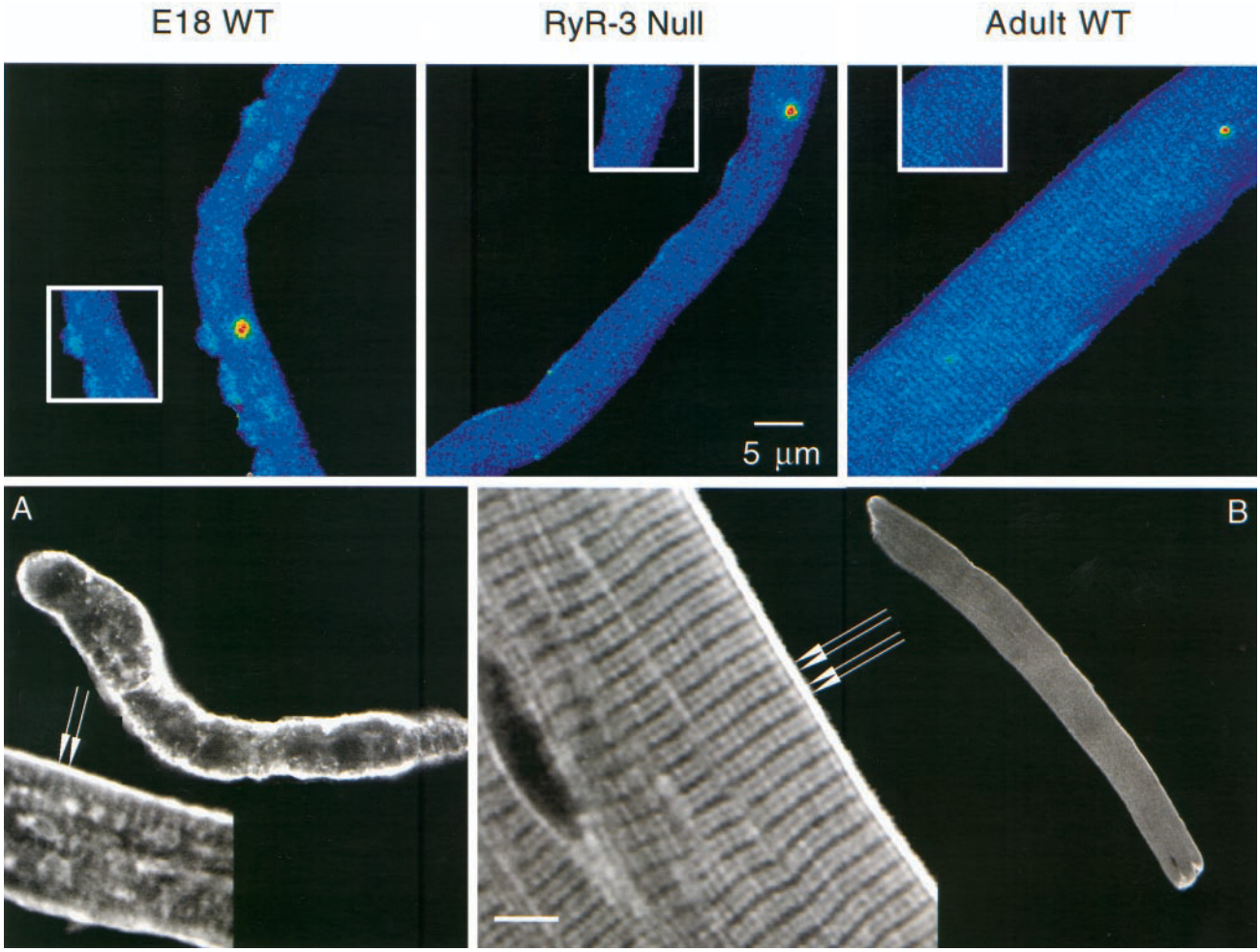

FIGURE 1 *Top panels* show confocal pseudocolor images of cells loaded with fluo-3 during a Ca^{2+} spark. Full-size images have a size of 512 × 512 pixels (0.2 × 0.2 microns per pixel) and were acquired at a rate of 1.2 s per image. Insets show the same area of the cell without the spark. An 8-pixel smoothing and a 32-color table were applied to highlight the location of the Ca^{2+} spark. Blue and red colors depict lower and higher fluorescence intensities, respectively. The 5-micron scale bar is the same for the three top images. Bottom panels show confocal gray-scale images of embryonic wt E18 cells dissociated from intercostal muscles *(A)*, and adult cells dissociated from the FDB muscle *(B)* stained with 4 μM of Di-8-ANNEPS. Insets show enlarged details of the developing and adult transverse tubular system. *Arrows* show nascent t-tubules in the embryonic cell *(A)* or parallel rows of t-tubules in the adult cell *(B)*. An 8-pixel smoothing and a 32-level gray scale were applied to highlight the Di-8-ANNEPS fluorescence. White color depicts high fluorescence intensity. The scale in the Di-8-ANNEPS images is 14 microns in *A*, 6 microns in the enlarged image of *A*, 60 microns in *B*, and 5 microns in the enlarged image of *B*.

lock et al., 1995). Embryonic wt cells (Fig. 1 *A*) and similarly RyR type 3-null cells (not shown) stained with Di-8 ANNEPS were >200 microns in full length and <25 microns in maximum width. Adult FDB cells (Fig. 1 *B*) were >500 microns in length and <75 microns in width. In embryonic myotubes, the bulk of the stain accumulated on the cell surface and in areas immediately adjacent to the cell surface. This staining pattern is consistent with the absence of a fully developed transverse tubular membrane system (t-system) at this stage of development (Franzini-Armstrong, 1991). Also shown in Fig. 1 *A* is a section of a different cell at a higher magnification, in which features of the nascent t-system are better appreciated. These features were present in some wt and knockout embryonic cells and consist of faint transverse-oriented threads near the cell surface (see arrows) as well as diffusely stained features in the cell center. Both are consistent with the irregular disposition of the t-system at this stage of development, part of which is composed of longitudinal membrane elements running in the interior of the cell (Franzini-Armstrong, 1991). In the adult cells, the dye accumulated on the surface and there was also a periodic staining in the interior. This is shown in a section of a cell at higher magnification in Fig. 1 *B*. The fluorescence pattern consisted of pairs of adjacent beaded lines (see pairs of arrows) with a much wider inter-pair spacing than intra-pair spacing. This pattern is entirely consistent with the anatomical disposition of the adult transverse tubular system, which in mammalian skeletal muscle consists of two rows of transverse tubules per sarcomere. In addition, this pattern is identical to the immunofluorescence staining pattern of the t-system of adult rabbit skeletal muscle (Rosemblatt et al., 1981).

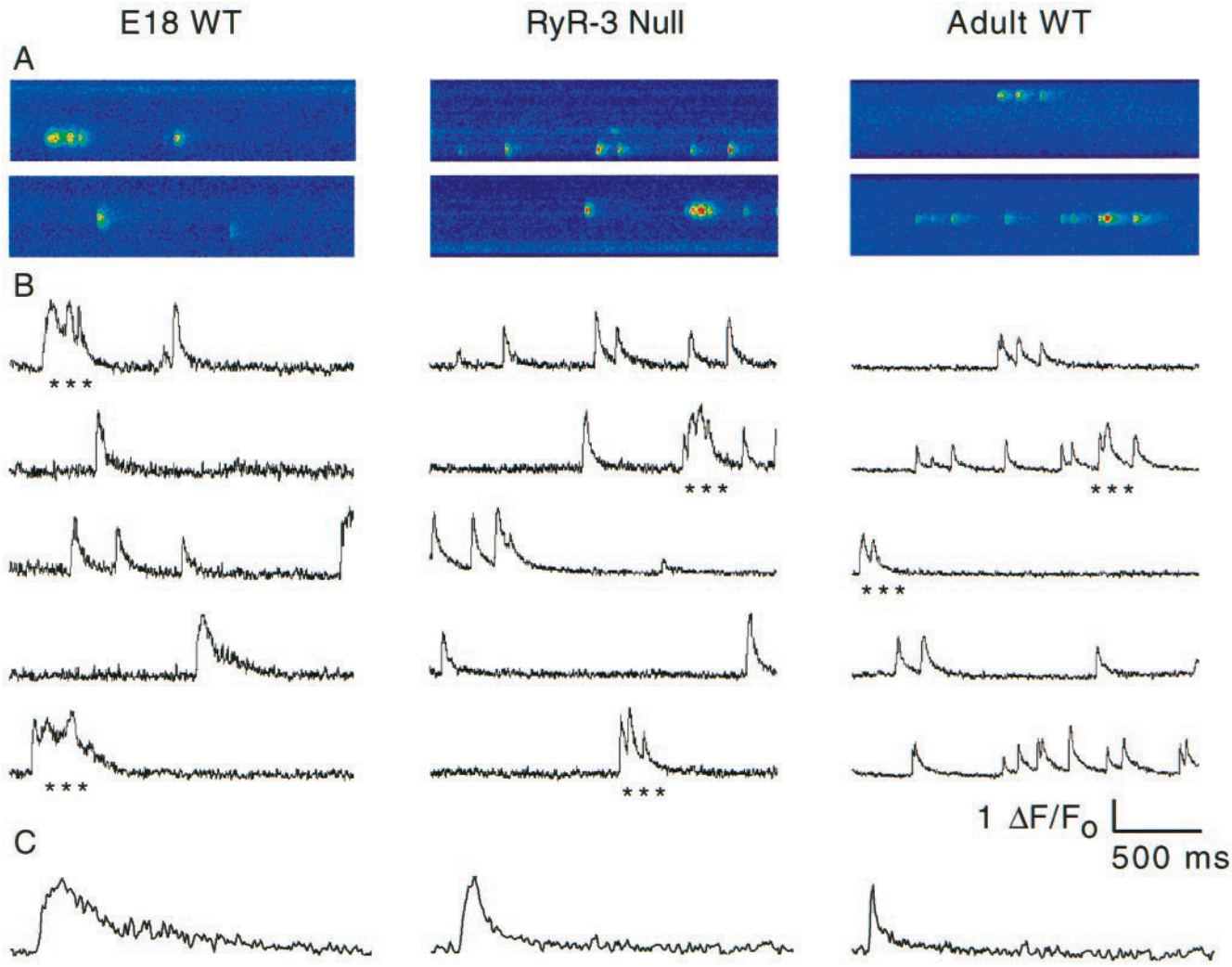

FIGURE 2 Ca^{2+} sparks in embryonic (E18 wt and RyR3-null) and adult wt myotubes. *A* shows confocal line-scan images of fluo-3 fluorescence from two separate sites of sparks each in a separate cell. All images have a size of 20 microns (*vertical*) × 2.05 s (*horizontal*) and a pixel size of 0.2 microns × 2.05 ms. *B* shows the time course of the change in fluorescence intensity during a spark obtained by integration of the line-scan fluorescence. The first and second traces correspond to the integrated fluorescence of the line-scan images shown in *A*. The asterisks indicate some sparks occurring in rapid succession that were not analyzed. *C* shows an expanded time course of typical sparks seen in each cell type. The fluorescence was scaled to the peak fluoresence and the time calibration bar shown in *B* is 250 ms in *C*.

Fig. 2 shows line-scan images (Fig. 2 *A*) of Ca^{2+} sparks in embryonic and adult cells. Time increases from left to right and the spatial dimension is vertical. Only the cell region covered by the spark is shown in the line-scan image. The images show that Ca^{2+} sparks occurred repetitively at the same location in cells, although the overall density of sparks per unit cell dimension was low. Considering those line-scans with at least one spark, the spark frequencies were in all cases less than 0.02 events/micron/second. This frequency is a small fraction of the spark frequency reported for depolarized cells but within the range of the resting spark frequency in frog fibers. The latter was reported to be ~0.18 events/triad/second or ~0.06 events/micron/second, given a triad spacing of 2.9 microns (Klein et al., 1996). Fig. 2 *B* shows several traces of fluorescence intensity as a function of time near the center of sparks. Ca^{2+} sparks in wt embryonic myotubes had a prolonged decay phase that has been described previously (Conklin et al., 1999a). The asterisks indicate examples of multiple events excluded from the analysis due to the summation of the signals. In most cases, sparks in RyR type 3-null myotubes of the same age had a much faster decay phase. This resulted in an overall shortening of the spark duration relative to wt counterparts. Consistent with a shorter spark duration, the spatial dimension of sparks in E18 RyR type 3-null myotubes was also reduced. Because RyR-3 is prominent in all embryonic skeletal muscles (Flucher et al., 1998) and is severely reduced in adult twitch muscle (Bertocchini et al., 1997), we searched for resting sparks in cells dissociated from the adult FDB foot muscle. We focused on the FDB muscle because healthy single cells may easily be obtained from the partially dissected FDB (Allard et al., 1996). In addition, these cells have the EC coupling characteristics of fast-twitch muscle fibers (Jacquemond, 1997; Csernoch et al., 1998). The most noticeable characteristic of sparks in FDB muscle cells was that the peak fluorescence was significantly lower than in either of the two embryonic cells. In addition, the decay phase in a significant fraction of the events was faster than in wt embryonic myotubes. This is better presented in Fig. 2 *C*, in which typical sparks encountered in each cell type were scaled to the peak fluorescence for comparison. The faster decay phase of sparks in FDB muscle resulted in an overall shortening of the mean half-duration and mean half-width. We also measured resting sparks in adult RyR type 3-null cells and found them to be remarkably similar to those of adult wt cells (not shown).

Histograms of the half-width (FWHM), the maximum fluorescence intensity ($\Delta F/Fo$), and the half-duration (FTHM) of individual sparks collected in wt E18 (280 events), RyR type 3-null E18 (368 events), and wt adult (220 events) cells are shown in Fig. 3. Sparks occurring in rapid succession at the same location for which the fluorescence did not decay to the baseline between events (see Fig. 2) were excluded from these distributions. For all three spark parameters, the distributions were much broader in wt embryonic cells than in the other two groups. The distributions in embryonic wt or RyR type 3-null cells were roughly symmetrical in the case of the half-width and asymmetric in the case of the peak intensity and half-duration. However, in neither case were these distributions bimodal. All three distributions of half-duration were skewed with a mean longer than the mode. Thus, brief events were clearly overrepresented in each of the three cell types. The population averages for each parameter and the time to peak fluorescence are shown in Table 1. Any two data sets with significantly different means are indicated. All parameters were smaller in wt adult than in embryonic cells. Furthermore, the spark parameters of embryonic RyR type 3-null cells were closer to those of adult cells than to those of wt cells. A better appreciation of the differences in spark parameters in embryonic and adult muscle cells was obtained in Fig. 4 by plotting the FWHM, $\Delta F/Fo$, and FTHM in three dimensions. The 3-D plots showed that in wt embryonic cells there was a broad tendency for Ca^{2+} sparks to increase in intensity and dimension in parallel with an increase in duration. Accordingly, the shape of the 3-D distributions was roughly that of a broad ellipsoid extending through the middle of the time dimension (*x-y*) plane and upwards in the intensity (*z*) axis. In RyR type 3-null myotubes, the half-duration of sparks was curtailed much more than the other two parameters. Consequently, the shape of the 3-D distribution was narrower and extended almost vertically into the *z* axis. In adult muscle, the means of all three parameters were reduced and their variations were more confined. In summary, these data showed that the specific absence of RyR type 3 significantly reduced the spatial and temporal properties of Ca^{2+} sparks in embryonic muscle. In addition, the parameters of embryonic RyR type 3-null cells were much closer to those of adult cells than to those of embryonic wt cells. Western blots using a highly specific RyR type 3 antibody (Bertocchini et al., 1997) showed that RyR type 3 protein in homogenates of the adult FDB muscle preparation were at least 10-fold lower than in the embryonic intercostal muscle preparation (not shown). This control convinced us that the decrease in Ca^{2+} spark parameters found in adult cells could be correlated with a decrease in RyR type 3 content of the adult FDB muscle.

We determined that sparks were mediated by RyR channels by treating cells with caffeine and tetracaine, which are known to affect RyRs and respectively stimulate and inhibit Ca^{2+} sparks in embryonic and adult muscle (Klein et al., 1996; Shirokova and Rios, 1997; Conklin et al., 1999a). Fig. 5 shows line-scans in cells during a control period (Fig. 5 *A*) and 30 min after addition of 0.2 mM of tetracaine to the bath solution (Fig. 5 *B*). This prolonged exposure to tetracaine resulted in a complete cessation of sparks, and the inhibition could not be reversed after extensive washing out of the anesthetic. To ensure that the loss of activity was not due to a loss in SR Ca^{2+}, we exposed the same cells to 0.1 mM caffeine or in the case of RyR type 3-null cells to 2 mM caffeine (Fig. 5 *C*). In the embryonic and adult wt cells there was an increase in line-scan fluorescence; however, the recovery of Ca^{2+} spark activity was difficult to assess under these conditions. In the adult cell, exposure to caffeine

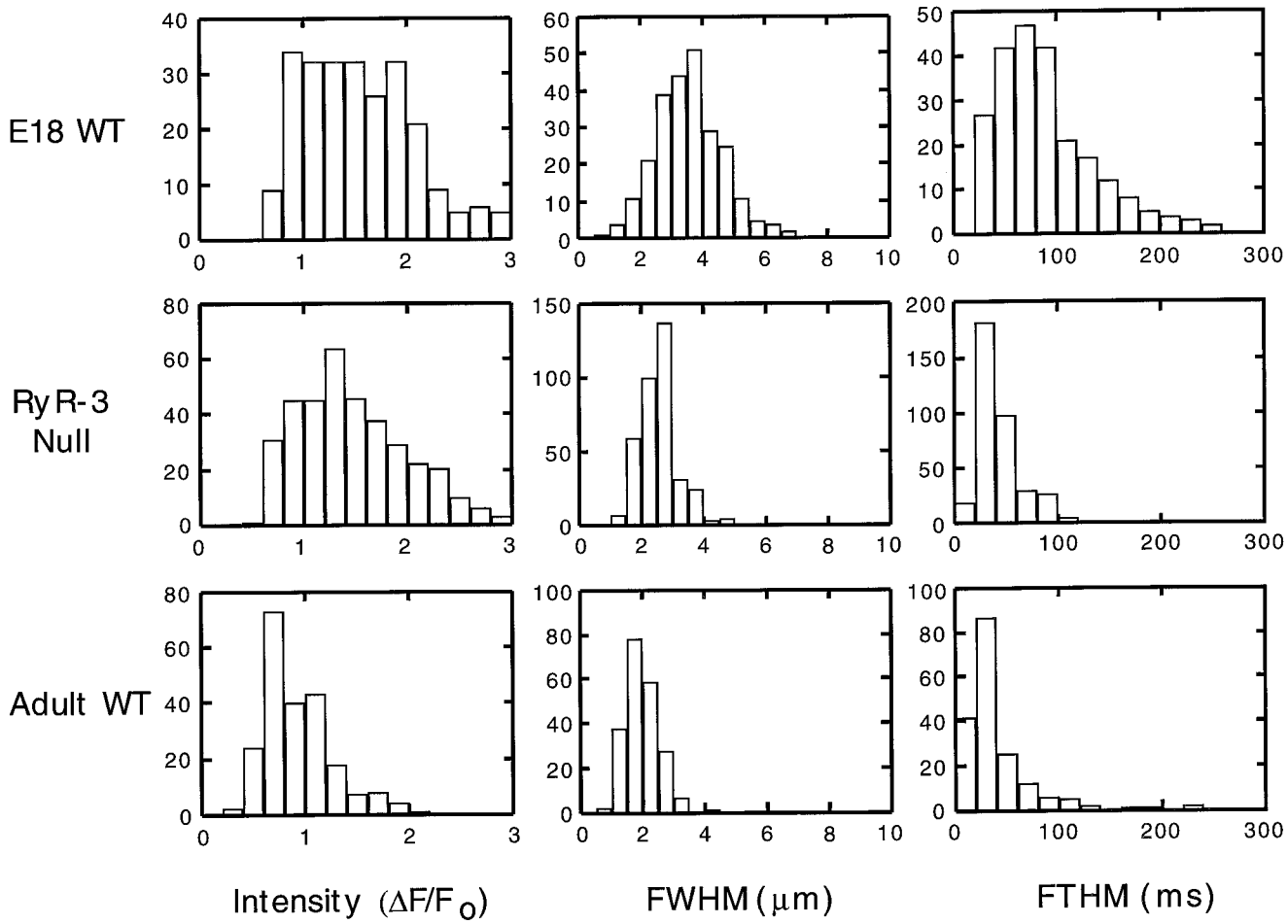

FIGURE 3 Histograms of Ca^{2+} spark size, intensity and duration. The peak fluorescence intensity in ΔF/Fo units, full width at half-maximal fluorescence intensity (FWHM), and full duration at half-maximal fluorescence intensity (FTHM), of sparks identified in wt E18 (280 events), RyR type 3 E18 (368 events) and adult cells (220 events) were sorted into bins. For each parameter, the bin scale is the same for all cell types. Note that the events scale is variable for the different cell types.

following treatment with tetracaine increased the cell fluorescence such that the sarcomere staining pattern was exposed. Consistent with previous results (Bertocchini et al., 1997), we found that RyR type 3-null cells were remarkably insensitive to caffeine. In these cells, 2 mM caffeine produced only a marginal increase in cell fluorescence, whereas the same concentration in either E18 or adult wt cells caused a global increase in cell fluorescence followed by cell movement (not shown). A direct stimulation of the spark fluorescence by caffeine in the absence of tetracaine is shown in Fig. 5, *D* and *E*, in a separate group of cells. To avoid large changes in resting fluorescence, we tested caffeine in the micromolar range. At 0.01 mM, caffeine produced an increase of the decay phase of the spark, which can be seen by comparing line-scans during the control period (Fig. 5 *D*) and >10 min into the test period (Fig. 5 *E*). This effect was readily observed in wt cells but was less obvious in the adult cells. In addition, there was no effect in RyR type 3-null cells consistent with the lack of an effect of caffeine in these cells in Fig. 5 *C*. Many sparks stimulated by caffeine in E18 wt cells had a characteristically long tail of fluorescence that increased the overall duration of the event. We quantified the effect of caffeine by monitoring sparks at the same site in a cell during control and test

TABLE 1 Parameters of Ca^{2+} sparks in embryonic and adult mammalian skeletal muscle

	ΔF/Fo	Time to peak (ms)	FTHM (ms)	FWHM (μm)
E18 WT (n = 280)	1.6 ± 0.6	42.8 ± 24	84.5 ± 46	3.5 ± 1.1
E18 RyR 3-null (n = 368)	1.5 ± 0.6**	19.2 ± 16*	44.5 ± 25*	2.6 ± 0.6*
Adult WT (n = 220)	0.9 ± 0.3*	16.4 ± 14*	40.3 ± 35*	2.0 ± 0.5*

Asterisks indicate statistical confidence $P < 0.05$ (*) or $P > 0.05$ (**) in an unpaired t-test against the same parameter in E18 wt cells. Only peak ΔF/Fo of sparks in E18 RyR-3 null cells was not significantly different from that of sparks in E18 wt cells.

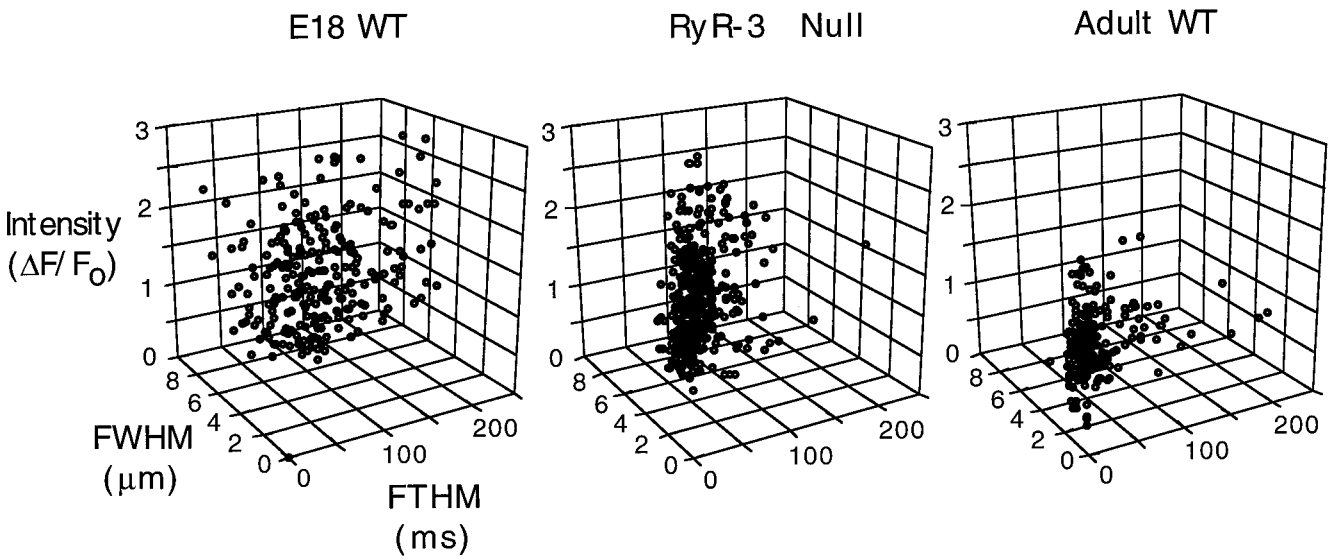

FIGURE 4 Relation of Ca^{2+} spark width to intensity and duration. The full duration at half-maximal fluorescence intensity FTHM (*x* axis), the full width at half-maximal fluorescence intensity FWHM (*y* axis), and the peak fluorescence intensity in ΔF/Fo units (*z* axis) of each spark in wt E18 (280 events), RyR type 3 E18 (368 events) and adult (220 events) cells are plotted in three dimensions.

periods. Caffeine was tested at a concentration of 0.01 mM and, in cells for which the resting fluorescence did not change significantly, up to 0.1 mM. At a single site in an E18 wt cell, the mean ΔF/Fo, FTHM, and FWHM were 2.0, 72 ms, and 3.1 microns, respectively, during the control period and increased to 2.2, 113 ms, and 3.5 microns, respectively, 15 min after exposure to 0.1 mM of caffeine. Averaged for three sites, the fold increase produced by micromolar caffeine in E18 wt cells were −1.1-fold for the peak ΔF/Fo, 2.9-fold for FTHM, and 1.6-fold for FWHM. The negative sign indicates that on average there was a slight decrease in peak fluorescence ratio after exposure to caffeine due to a slight increase in resting fluorescence. In the adult cells, micromolar caffeine produced only a modest increase in the spark duration with an average increase in FTHM of 1.5-fold. In RyR type 3-null cells, the spark parameters were unaffected by micromolar caffeine. We did not detect an increase in event frequency, which in adult cells has been shown to occur at a much higher caffeine concentration (Klein et al., 1996). The effect of tetracaine and caffeine showed that Ca^{2+} sparks in embryonic muscle were mediated by RyR channels.

DISCUSSION

During the late gestation period, RyR type 3 is widely expressed in limb muscles (tibialis anterior, extensor digitorum longus, soleus, biceps, and triceps femoris), abdominal muscles, and the diaphragm (Bertocchini et al., 1997). During the neonatal phase, RyR type 3 expression is drastically reduced, whereas in the adult musculature, this isoform is confined almost exclusively to the diaphragm (Bertocchini et al., 1997). In the adult diaphragm, RyR type 3 accounts for a small fraction of the total RyR protein (Jeyakumar et al., 1998). Based on the pattern of RyR type 3 expression, we assessed the contribution of RyR type 3 to Ca^{2+} sparks by focusing on fast-twitch intercostal muscles from late gestation control (wt) and RyR type 3-null mice. In addition, to provide an internal reference for the kinetics of sparks in RyR type 3-null cells, we searched for Ca^{2+} sparks in well-characterized adult FDB muscle (Jacquemond, 1997; Csernoch et al., 1998). Controls showed that immunodetectable levels of RyR type 3 in adult FBD were severely reduced (>10-fold) compared to those in embryonic skeletal muscles (not shown). To our knowledge, this is the first report of Ca^{2+} sparks in adult mammalian muscle cells. Ca^{2+} sparks in embryonic RyR type 3-null myotubes were significantly smaller, with a faster time to peak and a shorter duration than sparks in wt muscle of the same age. This result showed that RyR type 3 contributes substantially to the kinetics and overall dimensions of Ca^{2+} sparks in embryonic muscle. The smaller sparks encountered in RyR type 3-null cells and the reduced amount of RyR type 3 in adult muscle provides a simple explanation of why the sparks in embryonic muscle were significantly larger and longer-lasting than the sparks in adult skeletal muscle described in this report. Finally, the data presented here make it abundantly clear that RyR type 1 alone can engage in Ca^{2+} spark activity in muscle cells.

The distributions of half-width, peak intensity, and half-duration of wt embryonic sparks were broad, with means larger than those reported in adult amphibian cells (Tsugorka et al., 1995; Klein et al., 1996). In principle, a large spark may be produced by the summation of two or more smaller events. Summation of events should produce multiple maxima in the distributions of spark parameters. Inspection of the histograms (Fig. 3) revealed many asymmetries in these distributions but no convincing evidence in

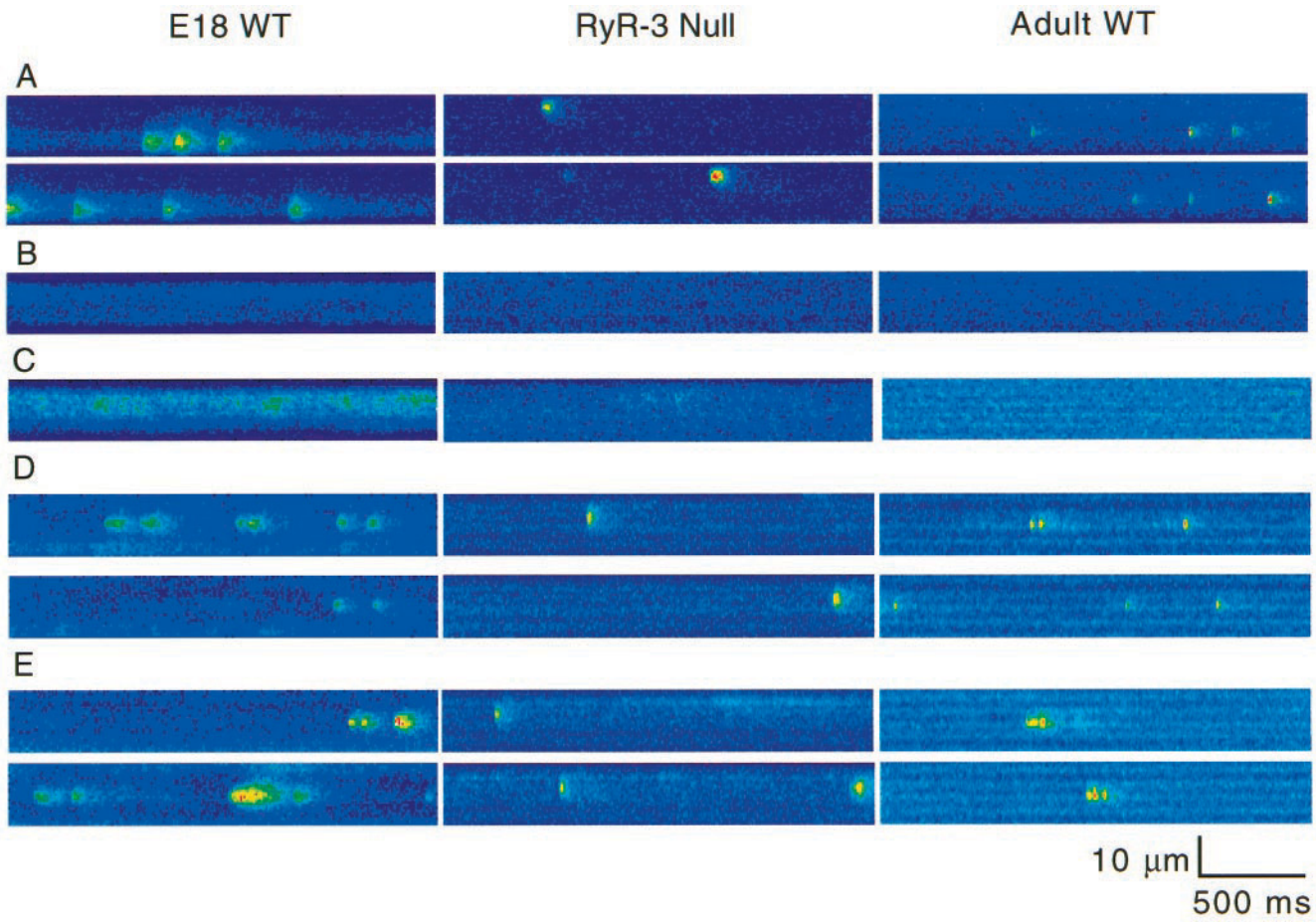

FIGURE 5 Ca^{2+} spark inhibition by tetracaine and stimulation by caffeine. All line-scan images have a dimension of 15 microns (vertical) and 2.05 s (horizontal). Line-scans in panels *A-C* are from the same cell (E18 WT, E18 RyR-3 null or adult WT) at the same location. *A* shows two line-scans at a site of sparks during the control period. *B* shows a line-scan 30 min after addition of tetracaine to the bath solution at a final concentration of 0.2 mM. *C* shows a line-scan after addition of caffeine at a final bath concentration of 0.1 mM in case of E18 wt and adult wt cells or 2 mM in case of the RyR type 3-null cell. Line-scans in panels *D* and *E* are from a separate group of cells. *D* shows two line-scans at the same site during the control period. *E* shows two line-scans at the same location >10 min after addition of caffeine to the bath solution at a final concentration of 0.01 mM.

favor of multiple maxima. Thus, we are inclined to believe that the ultimate explanation for the large size of embryonic sparks may reside elsewhere. Numerous alternative possibilities were recently discussed (Conklin et al., 1999a). On the other hand, it was reassuring to find that the resting Ca^{2+} sparks identified in adult FDB muscle were similar to those previously identified in adult amphibian skeletal muscle. Spontaneous Ca^{2+} sparks in adult amphibian skeletal muscle had the same characteristics at all potentials, including a peak $\Delta F/Fo$ of ~1, a half-duration of ~15 ms, and a FWHM of ~1.5 microns (Lacampagne et al., 1996). In the present study, adult resting sparks had a $\Delta F/Fo$ of ~0.9 and a FWHM of ~2 microns (Table 1). However, the half-time of the events in our study was close to 40 ms (Table 1). It should be pointed that in the present study, the half-duration of sparks in FDB muscle were broadly distributed, with about one-third of the events lasting 20 ms or less. In addition, the present measurements were performed in intact cells, whereas those in amphibian skeletal muscle were performed in cells dialyzed with solutions in an effort to stabilize the cytosolic Ca^{2+}. In this respect, it is significant to note that studies in amphibian muscle that use Ca^{2+}-EGTA buffers prepared with millimolar concentrations of EGTA (Shirokova et al., 1997, 1998) have consistently reported spark lifetimes shorter than those reported for experiments using submillimolar EGTA (Klein et al., 1996; Lacampagne et al., 1996). Thus, the Ca^{2+}-buffering capacity of the internal solution used for cell dialysis could also be a significant factor in determining the Ca^{2+} spark kinetics.

RyR type 3 colocalizes with RyR type 1 at junctional triads, forming clusters in which both isoforms are present (Flucher et al., 1998; Protasi et al., 1999). However, the functional roles of RyR type 1 and RyR type 3 in triadic junctions must be fundamentally different, because RyR type 3 channels cannot be activated by the membrane potential (Sorrentino and Reggiani, 1999). We speculate that in embryonic skeletal muscle cells, RyR type 3 increases the density of junctional RyR channels that can be activated by Ca^{2+}. Thus, the density of Ca^{2+}-activated RyR channels may be much higher in a wt embryonic cell than in a RyR

type 3-null cell and certainly higher in wt embryonic cells than in most adult cells. The higher density of Ca^{2+}-activated RyRs may be the fundamental reason why Ca^{2+} sparks of embryonic cells have parameters larger than those of adult cells (Table 1). In clusters of RyR type 1 and RyR type 3 channels, RyR type 3 channels could increase the dimensions of Ca^{2+} sparks by one of several mechanisms. The total Ca^{2+} contributed by RyR type 3 to the spark is a function of the product iNp, where i is single channel current, N is the is the total number of channels, and p is the open probability of a single channel. RyR type 3 could increase the ensemble average open probability of RyR channels in the cluster or could contribute to increase the number of RyRs simultaneously open during the elementary Ca^{2+} release event. However, the contribution of i may be less significant because the single channel current of RyR type 1 and type 3 channels is similar (Percival et al., 1994; Chen et al., 1997; Sonnleitner et al., 1998). A potential contribution of the Np product to the spark kinetics is supported by recordings of RyR type 3 channels in planar bilayers. Avian skeletal muscle is endowed with α and β RyR isoforms, of which β was shown to be homologous to mammalian RyR type 3 (Ottini et al., 1996). Under the same ligand conditions, 60% of the openings of chick β RyR channels are approximately 50-fold longer than the bulk of the openings of chick α RyR channels (Percival et al., 1994). β RyR channels also remain open over a wider range of cytoplasmic Ca^{2+} and, in the presence of ATP, they are not inactivatable by Ca^{2+} (Percival et al., 1994). A long mean open time has also been reported in the mammalian RyR type 3 channel (Chen et al., 1997). This result and the low sensitivity of mammalian RyR type 3 to inactivation by Ca^{2+} (Sonnleitner et al., 1998) and by Mg^{2+} (Murayama and Ogawa, 1997) suggest that RyR type 3 channel in situ could remain open for longer periods than RyR type 1 channels. These long-lasting openings arising from RyR type 3 channels could increase the Ca^{2+} release flux during a spark and thus prolong the spark duration and half-width. The activities of these long-lasting open channels could overlap in time and this could result in positive reinforcement of the Ca^{2+} flux during a spark. In summary, the known subcellular distribution and ligand gating characteristics of RyR type 3 channels in skeletal muscle are entirely supportive of the present observation that RyR type 3 enlarges Ca^{2+} sparks.

A recent report showed the absence of Ca^{2+} sparks activated by voltage in internally dialyzed muscle fibers from rat EDL (Shirokova et al., 1998) and suggested that in mammalian skeletal muscle, global Ca^{2+} transients are not produced by summation of Ca^{2+} sparks. By implication, the resting sparks reported here may serve purposes other than participation in excitation-contraction coupling. Alternatively, it is possible that sparks in mammalian muscle may be more labile than their counterparts in amphibian muscle and that critical cytosolic factors may be lost during dialysis. Even if this report is taken at face value, there are many processes critical for myogenesis that could be influenced by resting Ca^{2+} sparks. For example, it has been shown that blockade of spontaneous Ca^{2+} transients from RyRs in *Xenopus* myocytes disrupts myosin thick filament (A band) assembly, an effect that can be mimicked in these cells by inhibition of an embryonic Ca^{2+}/calmodulin-dependent myosin light chain kinase (Ferrari et al., 1998). In addition, local spontaneous Ca^{2+} spikes and waves at specific frequencies in developing *Xenopus* spinal neurons regulate the expression of a delayed rectifier potassium current as well as the normal appearance of GABA immunoreactivity (Gu and Spitzer, 1995). In some neurons in culture, elementary Ca^{2+} release signals arose in part from clusters of RyRs (Koizumi et al., 1999). Hence, Ca^{2+} sparks could play a significant role in cell signaling in resting muscle cells and neurons. The contribution of RyR type 3 in triggering these crucial developmental processes remains to be investigated.

Supported by National Institutes of Health HL47053 (R. C.), American Heart Association Wisconsin Affiliate Predoctoral Fellowship (M. C.), and Telethon grant no. 1151 (V. S.).

REFERENCES

Allard, B., J. C. Bernengo, O. Rougier, and V. Jacquemond. 1996. Intracellular Ca^{2+} changes and Ca^{2+}-activated K+ channel activation induced by acetylcholine at the end plate of mouse skeletal muscle fibers. *J. Physiol. (Lond.)* 460:1–13.

Barone, V., F. Bertocchini, R. Bottinelli, F. Protasi, P. D. Allen, C. Franzini-Armstrong, C. Reggiani, and V. Sorrentino. 1998. Contractile impairment and structural alterations of skeletal muscles from knock-out mice lacking type-1 and type-3 ryanodine receptors. *FEBS Lett.* 422: 160–164.

Bertocchini, F., C. E. Ovitt, A. Conti, V. Barone, H. R. Scholer, R. Bottinelli, C. Reggiani, and V. Sorrentino. 1997. Requirement for the ryanodine receptor type 3 for efficient contraction in neonatal skeletal muscles. *EMBO J.* 16:6956–6963.

Block, B., A., T. Imagawa, K. P. Campbell, and C. A. Franzini-Armstrong. 1988. Structural evidence for direct interaction between the molecular components of the transverse tubule/sarcoplasmic reticulum junction in skeletal muscle. *J. Cell Biol.* 107:2587–2600.

Chen, S. R. W., X. Li, K. Ebisawa, and L. Zhang. 1997. Functional characterization of the recombinant type 3 Ca^{2+} release channel (ryanodine receptor) expressed in HEK292 cells. *J. Biol. Chem.* 272: 24234–24246.

Cheng, H., W. J. Lederer, and M. B. Cannell. 1993. Calcium sparks: Elementary events underlying excitation-contraction coupling in heart muscle. *Science.* 262:740–744.

Conklin, M., P. Powers, R. G. Gregg, and R. Coronado. 1999a. Ca^{2+} sparks in embryonic mouse skeletal muscle selectively deficient in dihydropyridine receptor α1S or β1 subunits. *Biophys. J.* 76:657–669.

Conklin, M., C. Strube, V. Sorrentino, and R. Coronado. 1999b. Contribution of ryanodine receptor type 3 to Ca^{2+} sparks in embryonic skeletal muscle. *Biophys. J.* 76:A386 (abstr.).

Conti, A., L. Gorza, and V. Sorrentino. 1996. Differential distribution of ryanodine receptor type 3 (RyR3) gene product in mammalian skeletal muscles. *Biochem. J.* 316:19–23.

Csernoch, L., C. Bernengo, P. Szentezi, and V. Jacquemond. 1998. Measurements of intracellular Mg^{2+} in mouse skeletal msucle fibers with the fluorescent indicator mag-indo-1. *Biophys. J.* 75:957–967.

Dietze, B., F. Bertocchini, V. Barone, A. Struk, V. Sorrentino, and W. Melzer. 1998. Voltage-controlled Ca^{2+} release in normal and ryanodine receptor type 3 (RyR3)-deficient mouse myotubes. *J. Physiol.* 513.1: 3–9.

Ferrari, M. B., K. Ribbeck, D. J. Hagler, and N. C. Spitzer. 1998. A calcium signaling cascade essential for myosin thick filament assembly in Xenopus myocytes. *J. Cell Biol.* 141:1349–1356.

Flucher, B. E., A. Conti, and V. Sorrentino. 1998. Type 3 ryanodine receptor is expressed in skeletal muscle triads of developing mice. *Biophys. J.* 74:A338 (abstr.).

Franzini-Armstrong, C. 1991. Simultaneous maturation of transverse tubules and sarcoplasmic reticulum during muscle differentiation in the mouse. *Dev. Biol.* 146:353–363.

Gu, X., and N. C. Spitzer. 1995. Distinct aspects of neuronal differentiation encoded by frequency of spontaneous Ca^{2+} transients. *Nature.* 375: 784–787.

Giannini, G., A. Conti, S. Mammarella, M. Scrobogna, and V. Sorrentino. 1995. The ryanodine receptor/calcium channel genes are widely and differentially expressed in murine brain and peripheral tissues. *J. Cell Biol.* 128:893–904.

Gyorke, S., P. Velez, B. Suarez-Isla, and M. Fill. 1994. Activation of single cardiac and skeleal ryanodine receptor channels by flash photolysis of caged Ca^{2+}. *Biophys. J.* 66:1879–1886.

Hakamata, Y., J. Nakai, H. Takeshima, and K. Imoto. 1992. Primary structure and distribution of a novel ryanodine receptor/calcium release channel from rabbit brain. *FEBS Lett.* 312:229–235.

Jacquemond, V. 1997. Indo-1 fluorescence signals elicited by membrane depolarization in enzymatically isolated mouse skeletal muscle fibers. *Biophys. J.* 73:920–928.

Jeyakumar, L. H., J. A. Copello, A. M. O'Malley, G.-M. Wu, R. Grassucci, T. Wagenknecht, and S. Fleischer. 1998. Purification and characterization of ryanodine receptor 3 from mammalian tissue. *J. Biol. Chem.* 273:16011–16020.

Klein, M. G., H. Cheng, L. F. Santana, Y.-H. Jiang, W. J. Lederer, and M .F. Schneider. 1996. Two mechanisms of quantized calcium release in skeletal muscle. *Nature.* 379:455–458.

Koizumi, S., M. D. Bootman, L. K. Bobanovic, M.J. Schell, M. J. Berridge, and P. Lipp. 1999. Charaterization of elementary Ca^{2+} release signals in NGF-differentiated PC12 cells and hippocampal neurons. *Neuron.* 22: 125–137.

Lacampagne, A., W. J. Lederer, M. F. Schneider, and M. G. Klein. 1996. Repriming and activation alter the frequency of stereotyped discrete Ca^{2+} release events in frog skeletal muscle. *J. Physiol.* 497.3:508–588.

Murayama, T., and Y. Ogawa. 1997. Characterization of type 3 ryanodine receptor (RyR3) of sarcoplasmic reticulum rabbit skeletal muscles. *J. Biol. Chem.* 272:24030–24037.

Ottini, L., G. Marziali, A. Conti, A. Charlesworth, and V. Sorrentino. 1996. Alpha and beta isoforms of ryanodine recpeotrs from chicken skeletal muscle are the homologues of mammalian RyR1 and RyR3. *Biochem. J.* 315:207–216.

Oyamada, H., Y. Murayama, T. Takagi, M. Iino, T. Miyata, Y. Ogawa, and M. Endo. 1994. Primary structure and distribution of ryanodine-binding protein isoforms of the bullfrog skeletal muscle. *J. Biol. Chem.* 269: 17206–17214.

Parker, I., W.-J. Zang, and W. G. Wier. 1996. Ca^{2+} sparks involving multiple Ca^{2+} release sites along Z-lines in rat heart cells. *J. Physiol.* 497.1:31–38.

Percival, A. L., A. J. Williams, J. K. Kenyon, M. M. Grinsell, J. A. Airey, and J. L. Sutko. 1994. Chicken skeletal muscle ryanodine receptor isoforms: ion channel properties. *Biophys. J.* 67:1834–1850.

Protasi, F., H. Takekura, Y. Wang, S. R. W. Chen, C. Franzini-Armstrong, and P. D. Allen. 1999. RyR3 expression in a dyspedic cell line does not restore junctional DHPR tetrads. *Biophys. J.* 76:A470 (abstr.).

Rosemblatt, M., C. Hidalgo, C. Vergara, and N. Ikemoto. 1981. Immunological and biochemical properties of transverse tubule membranes isolated from rabbit skeletal muscle. *J. Biol. Chem.* 256:8140–8148.

Shacklock P. S., W. G. Wier, and C. W. Balke. 1995. Local calcium transients (Ca^{2+} sparks) originate at transverse tubules in rat heart cells. *J. Physiol.* 487:601–608.

Shirokova, N., and E. Rios. 1997. Small event Ca^{2+} release: a probable precursor of Ca^{2+} sparks in frog skeletal muscle. *J. Physiol.* 502.1:3–11.

Shirokova, N., J. Garcia-Martinez, and E. Rios. 1998. Local calcium release in mammalian skeletal muscle. *J. Physiol.* 512.2:377–384.

Sonnleitner, A., A. Conti, F. Bertocchini, H. Schindler, and V. Sorrentino. 1998. Functional properties of the ryanodine receptor type 3 (RyR3) Ca^{2+} release channel. *EMBO J.* 17:2790–2798.

Sorrentino, V., and C. Reggiani. 1999. Expression of Ryanodine receptor type 3 in skeletal muscle: a new partner in excitation-contraction coupling? *Trends Cardiovasc. Med.* 9:53–60.

Strube, C., M. Beurg, P. A. Powers, R. G. Gregg, and R. Coronado. 1996. Reduced Ca^{2+} current, charge movement, and absence of Ca^{2+} transients in skeletal muscle deficient in dihydropyridine receptor beta-1 subunit. *Biophys. J.* 71:2531–2543.

Sutko, J. L., and J .A. Airey. 1996. Ryanodine receptor Ca^{2+} release channels: does diversity in form equals diversity in function? *Physiol. Rev.* 76:1027–1071.

Takeshima, H., I. Masamitsu, H. Takekura, M. Nishi, J. Kuno, O. Minowa, H. Takano, and T. Noda. Excitation-contraction uncoupling, and muscular degeneration in mice lacking functional skeletal muscle ryanodine-receptor gene. 1994. *Nature.* 369:556–559.

Takeshima, H., T. Yamazawa, T. Ikemoto, H. Takekura, M. Nishi, T. Noda, and M. Iino. 1995. Ca^{2+}-induced Ca^{2+} release in myocytes from dyspedic mice lacking the type-1 ryanodine receptor. *EMBO J.* 14: 2999–3006.

Takeshima, H., T. Ikemoto, M. Nishi, N. Nishiyama, M. Shimuta, Y. Sugitani, J. Kuno, I. Saito, H. Saito, M. Endo, M. Iino, and T. Noda. 1996. Generation and characterization of mutant mice lacking ryanodine receptor type 3. *J. Biol. Chem.* 271:19649–19652.

Tsugorka, A., E. Rios, and L. A. Blatter. 1995. Imaging elementary events of calcium release in skeletal muscle cells. *Science.* 269:1723–1726.

Yamazawa, T., H. Takeshima, M. Shimuta, and M. Iino. 1997. A region of the ryanodine receptor critical for excitation-contraction coupling in skeletal muscle. *J. Biol. Chem.* 272:8161–8164.